Fast Orthonormal Propagator Direction-Finding Algorithm Based on Fourth-Order Cumulants

Heping Shi, Wen Leng, Anguo Wang, Hua Chen, and Yuchu Ji

School of Electronic Information Engineering
Tianjin University, Tianjin 300072, China
shiheping@tju.edu.cn, lengwen@tju.edu.cn, agwang@tju.edu.cn, dkchenhua@tju.edu.cn, jiyuchu@126.com

Abstract ─ In this paper, a low complexity approach called modified fourth-order cumulants orthonormal propagator method (MFOC-OPM) is proposed for direction-of-arrival (DOA) estimation of incident narrowband signals impinging on a uniform linear array (ULA). In the proposed algorithm, the modified fourth-order cumulants (MFOC) matrix is achieved via removing the redundant information encompassed in the primary fourth-order cumulants (FOC) matrix, and then the direction-of-arrivals (DOAs) estimation of source signals can be resolved by exploiting the orthonormal propagator method (OPM). Without any spectrum-peak searching and eigenvalue decomposition (EVD) of the MFOC matrix, the theoretical analysis coupled with simulation results show that in comparison with the MFOC-MUSIC algorithm, the resultant algorithm can reduce computational complexity significantly, as well as yield good estimation performance in both spatially-white noise and spatially-color noise environments.

Index Terms ─ Direction-of-arrival (DOA), fourth-order cumulants (FOC), orthonormal propagator method (OPM), spatially-color noise, spatially-white noise.

I. INTRODUCTION

Over the past two decades, the issue of finding the direction-of-arrival (DOA) of source signals has received considerable attention in array signal processing fields such as radar, sonar, underwater acoustics, radio astronomy, speaker localization, mobile communication systems and wireless communication systems [1-2]. The classical high-resolution subspace algorithms for direction-of-arrivals (DOAs) estimation, such as multiple signal classification (MUSIC) [3-4] and estimation of signal parameters via rotation invariance techniques (ESPRIT) [5-6] algorithms, have provided satisfactory performance. Because these subspace-based algorithms break through the limitation of the Rayleigh, the super resolution DOAs estimation of the radiation sources can be achieved [7-8]. However, the aforementioned algorithms are not only sensitive to the noise, but also require a priori information of the noise. In addition, these algorithms employ either the eigenvalue decomposition (EVD) or singular value decomposition (SVD) to obtain the signal subspace and the noise subspace. Therefore, the computational complexity of these subspace-based algorithms is high especially when the number of sensors and snapshots is relatively large. This indicates that these conventional high-resolution algorithms might not be useful when the low-computational cost and highly real-time data process are required.

To alleviate aforesaid drawbacks, various useful algorithms have been proposed. Fortunately, the fourth-order cumulants (FOC) are asymptotically insensitive to Gaussian noise. Therefore, FOC have been shown to be a promising substitute for second-order statistic (SOS) in solving DOA estimation, since it is not necessary to know or to estimate the noise covariance as long as the noise is normally distributed [9-10], which is a reasonable assumption in practical situations. In order to reduce computational complexity, the propagator method (PM) in [11-12] and its improved algorithm called orthonormal propagator method (OPM) [13] are presented. The OPM executes a linear operator instead of EVD or SVD to obtain the signal subspace and the noise subspace, which can decrease the computational complexity effectively. Moreover, the OPM can obtain the same estimation performance as the high-resolution subspace-based algorithms but more efficient in computation in medium and high signal-to-noise ratio (SNR) conditions. An OPM-like (FOC-OPM) algorithm [14], based on FOC, is proposed to achieve good estimation performance. However, the computational complexity of this method is high since a great number of redundant information is contained in the FOC matrix. In [15], the authors considered the redundancy among the FOC matrix through analyzing the effective array aperture, which can increase the computational complexity greatly. Moreover, due to the finite sampling snapshots, there exists an estimation error between the FOC statistical matrix of the array received signal and its ideal matrix, thus the capacity of DOA estimation degrades.

Submitted On: April 3, 2013
Accepted On: December 10, 2014

In this paper, a novel MFOC-OPM algorithm is presented. The emphasis of this paper is on the investigation of the computational load. In the presented algorithm, the reduced-rank FOC matrix is obtained by removing the redundant information encompassed in the primary FOC matrix. Meanwhile, the effective extended aperture of the virtual array keeps unchanged for improving estimation performance. Then the DOAs estimation of source signals can be estimated by using the OPM to reduce computational complexity. Compared with the MFOC-MUSIC method in [16], the proposed algorithm not only has the advantages of good performance but also the reduction of computation.

The rest of the paper is organized as follows. The signal model is briefly introduced in Section II. The proposed algorithm is discussed in detail in Section III. In Section IV, simulation results are presented to verify the effectiveness of the proposed algorithm. Finally, some concluding remarks are made in Section V.

For the purpose of description, the following notations are used. Boldface italic lower/upper case letters denote vectors/matrices. $(\cdot)^*$, $(\cdot)^T$ and $(\cdot)^H$ stand for the conjugation, transpose and conjugate transpose of a vector/matrix, respectively. The notation E(x), *cum*(x) and $\otimes$ separately denote the expectation operator, the cumulants, and the Kronecker product, respectively.

II. SIGNAL MODEL

Consider M narrowband far-field plane wave sources $s_l(t)$, (l=1,…,M) impinging on a uniform linear array (ULA) with N identical omni-directional sensors, where the inter-element spacing is half of the wavelength. Assume that the source signals are stationary and mutually independent. The noise is the additive white/color Gaussian one, and statistically independent of the sources. Let the first sensor of the ULA be the reference, and then the observed data received by the kth sensor can be expressed as:

$$x_k(t)=\sum_{i=1}^{M}a_k(\theta_i)s_i(t)+n_k(t),\quad k=1,\cdots,N, \tag{1}$$

where $s_l(t)$ is the ith source, $n_k(t)$ is the Gaussian noise at the kth sensor and $\alpha_k(\theta_i)$ is the response of kth sensor corresponding to the ith source;

$$a_k(\theta_i)=\exp(j2\pi(d/\lambda)k\sin\theta_i), \tag{2}$$

where λ is the central wavelength, d is the spacing between two adjacent sensors. Thus, one column vector, which contains all the observed data received by N sensors, can be achieved:

$$\begin{aligned}\begin{bmatrix}x_1(t)\\x_2(t)\\\vdots\\x_N(t)\end{bmatrix}&=\begin{bmatrix}1&1&\cdots&1\\\exp(j\alpha_1)&\exp(j\alpha_2)&\cdots&\exp(j\alpha_M)\\\vdots&\vdots&\ddots&\vdots\\\exp(j(N-1)\alpha_1)&\exp(j(N-1)\alpha_2)&\cdots&\exp(j(N-1)\alpha_M)\end{bmatrix}\begin{bmatrix}s_1(t)\\s_2(t)\\\vdots\\s_M(t)\end{bmatrix}+\begin{bmatrix}n_1(t)\\n_2(t)\\\vdots\\n_N(t)\end{bmatrix}\\&=\begin{bmatrix}\boldsymbol{a}(\alpha_1)&\boldsymbol{a}(\alpha_2)&\cdots&\boldsymbol{a}(\alpha_M)\end{bmatrix}\begin{bmatrix}s_1(t)\\s_2(t)\\\vdots\\s_M(t)\end{bmatrix}+\begin{bmatrix}n_1(t)\\n_2(t)\\\vdots\\n_N(t)\end{bmatrix},\end{aligned} \tag{3}$$

where α_i=exp($2\pi(d/\lambda)sin\theta_i$). Therefore, the matrix form of (3) can be modeled as:

$$\boldsymbol{X}(t)=\boldsymbol{A}\boldsymbol{S}(t)+\boldsymbol{N}(t), \tag{4}$$

where $\boldsymbol{X}(t)=[x_1(t),\ldots,x_N(t)]^T$ is the $N\times1$ array output vector, $\boldsymbol{S}(t)=[s_1(t),\ldots,s_M(t)]^T$ is the $M\times1$ source vector, $\boldsymbol{A}=[\boldsymbol{a}(\theta_1),\ldots,\boldsymbol{a}(\theta_M)]$ is the $N\times M$ array manifold matrix and $\boldsymbol{N}(t)=[n_1(t),\ldots,n_N(t)]^T$ denotes the $N\times1$ complex Gaussian noise vector.

Assume that the source signals are zero-mean stationary random process, the FOC can be defined as:

$$\begin{aligned}cum(k_1,k_2,k_3^*,k_4^*)=&E(x_{k_1}(t)x_{k_2}(t)x_{k_3}^*(t)x_{k_4}^*(t))-\\&E(x_{k_1}(t)x_{k_3}^*(t))E(x_{k_2}(t)x_{k_4}^*(t))-\\&E(x_{k_1}(t)x_{k_4}^*(t))E(x_{k_2}(t)x_{k_3}^*(t))-\\&E[x_{k_1}(t)x_{k_2}(t)]E[x_{k_3}^*(t)x_{k_4}^*(t)]\\&k_1,k_2,k_3,k_4\in[1,\cdots,N],\end{aligned} \tag{5}$$

where $x_{k_m}(m=1,2,3,4)$ is the stochastic process. Apparently, $cum(k_1,k_2,k_3^*,k_4^*)$ has N^4 values with the change of k_1,k_2,k_3,k_4. For simplicity, equation (5) can be collected in matrix form, which is denoted by cumulants matrix $\boldsymbol{C}_4$. Therefore, the N^4 values can be stored in the $N^2\times N^2$ matrix $\boldsymbol{C}_4$, and $cum(k_1,k_2,k_3^*,k_4^*)$ appears as the $[(k_1\text{-}1)N+k_2]$th row and $[(k_3\text{-}1)N+k_4]$th column of $\boldsymbol{C}_4$;

$$\begin{aligned}&\boldsymbol{C}_4[(k_1-1)N+k_2,(k_3-1)N+k_4]\\&=cum(k_1,k_2,k_3^*,k_4^*)\\&=cum(\sum_{l=1}^{M}\boldsymbol{a}_l(k_1)s_l(t),\sum_{l=1}^{M}\boldsymbol{a}_l(k_2)s_l(t),\sum_{l=1}^{M}\boldsymbol{a}_l(k_3^*)s_l(t),\\&\quad\sum_{l=1}^{M}\boldsymbol{a}_l(k_4^*)s_l(t))+cum(n_{k_1}(t),n_{k_2}(t),n_{k_3^*}(t),n_{k_4^*}(t))\\&=cum(\sum_{l=1}^{M}\boldsymbol{a}_l(k_1)s_l(t),\sum_{l=1}^{M}\boldsymbol{a}_l(k_2)s_l(t),\sum_{l=1}^{M}\boldsymbol{a}_l(k_3^*)s_l(t),\\&\quad\sum_{l=1}^{M}\boldsymbol{a}_l(k_4^*)s_l(t))\\&=\sum_{l=1}^{M}\sum_{m=1}^{M}\sum_{i=1}^{M}\sum_{j=1}^{M}\boldsymbol{a}_l(k_1)\boldsymbol{a}_m(k_2)\boldsymbol{a}_i(k_3^*)\boldsymbol{a}_j(k_4^*)\\&\quad cum(s_l(t)s_m(t)s_i(t)s_j(t))\\&=\sum_{l=1}^{M}\boldsymbol{a}_l(k_1)\boldsymbol{a}_l(k_2)\boldsymbol{a}_l(k_3^*)\boldsymbol{a}_l(k_4^*)\\&\quad cum(s_l(t)s_l(t)s_l(t)s_l(t))\\&=\boldsymbol{B}\boldsymbol{C}_s\boldsymbol{B}^H,\end{aligned} \tag{6}$$

where $\boldsymbol{B}$ and $\boldsymbol{C}_s$ represent the extended array manifold and the FOC matrix of incident source signals, respectively. $\boldsymbol{B}=\boldsymbol{A}\otimes\boldsymbol{A}$, and each column of $\boldsymbol{B}$ is $\boldsymbol{b}(\theta)=\boldsymbol{a}(\theta)\otimes\boldsymbol{a}(\theta)$. It is obvious that $\boldsymbol{b}(\theta)$ is a $N^2\times1$ vector, which means that the array aperture of ULA is extended. That is, the number of resolved source signals is no less than that of sensors.

III. THE PROPOSED ALGORITHM

A. The effective array aperture extended

As proven in [17], an array of N arbitrary identical omni-directional sensors can be extended to at most of

N^2-N+1. Especially, the number of virtual elements is 2N-1 for ULA according to [17]. In order to discuss the effective aperture of ULA, three real elements (N=3) are considered, and $\boldsymbol{b}(\theta)$ can be expressed in detail as follows:

$$\begin{aligned}\boldsymbol{b}(\theta) &= \boldsymbol{a}(\theta) \otimes \boldsymbol{a}(\theta) \\ &= [1, z, z^2]^T \otimes [1, z, z^2]^T \\ &= [1, z, z^2, z, z^2, z^3, z^2, z^3, z^4]^T,\end{aligned} \tag{7}$$

where $z=exp(j2\pi(d/\lambda)sin\theta)$ and $\boldsymbol{a}(\theta)=[1, z, z^2]$. Equation (7) shows that there is a lot of redundancy in expanded steering vector $\boldsymbol{b}(\theta)$. That is, only from 1th to Nth and all kNth (k=2,...,N) items of the $\boldsymbol{b}(\theta)$ are valid, while others are redundant ones. In order to eliminate these repetitive elements, a (2N-1)×(2N-1) matrix $\boldsymbol{R}_4$ is firstly defined. Next, the 1th to Nth and all kNth (k=2,...,N) rows of $\boldsymbol{C}_4$ are taken out in sequence, and then store these rows in the 1th to (2N-1)th row of the new matrix $\boldsymbol{R}_4$. The same operation is performed on the 1th to Nth and all kNth (k=2,...,N) columns of $\boldsymbol{C}_4$ to obtain the 1th to (2N-1)th columns of $\boldsymbol{R}_4$. Similar to equation (6), $\boldsymbol{R}_4$ can be expressed as:

$$\begin{aligned}\boldsymbol{R}_4 &= \sum_{l=1}^{M}\sum_{m=1}^{M}\sum_{i=1}^{M}\sum_{j=1}^{M} \boldsymbol{d}_l(k_1)\boldsymbol{d}_m(k_2)\boldsymbol{d}_i(k_3^*)\boldsymbol{d}_j(k_4^*) \\ &\quad cum(s_l(t)s_m(t)s_i(t)s_j(t)) \\ &= \sum_{l=1}^{M} \boldsymbol{d}_l(k_1)\boldsymbol{d}_l(k_2)\boldsymbol{d}_l(k_3^*)\boldsymbol{d}_l(k_4^*) \\ &\quad cum(s_l(t)s_l(t)s_l(t)s_l(t)) \\ &= \boldsymbol{D}\boldsymbol{C}_s\boldsymbol{D}^H,\end{aligned} \tag{8}$$

where $\boldsymbol{D}$ denotes the extended array manifold without redundancy, and each column of $\boldsymbol{D}$ has the form of $\boldsymbol{d}(\theta)=[1,z,...,z^{2N-2}]^T$. Therefore, the reduced-dimension $\boldsymbol{R}_4$ not only contains all of the information about the original matrix $\boldsymbol{C}_4$, but also keeps the extended array aperture unchanged.

B. The MFOC-OPM algorithm

In practical applications, the actual $\boldsymbol{C}_4$ cannot be achieved. Therefore, we have to estimate $\hat{\boldsymbol{C}}_4$ from the received data by array measurements. Instead, we utilize the estimated value $\hat{\boldsymbol{R}}_4$ in place of $\boldsymbol{R}_4$, and then the DOAs estimation can be achieved by performing OPM on the $\hat{\boldsymbol{R}}_4$. Under the assumption of the independent sources, since $\boldsymbol{D}$ is a Vandermonde matrix as long as θ_i comes from M different directions, the matrix $\boldsymbol{D}$ is column full rank. That is, only M rows of the matrix $\boldsymbol{D}$ are linearly independent, and the remaining rows of matrix $\boldsymbol{D}$ can be expressed as a linear combination of the M rows. Without loss of generality, assume that the first M rows of matrix $\boldsymbol{D}$ are linear independent, and then the matrix $\boldsymbol{D}$ can be partitioned as follows:

$$\boldsymbol{D} = \begin{bmatrix}\boldsymbol{D}_1 \\ \boldsymbol{D}_2\end{bmatrix}, \tag{9}$$

where the dimension of $\boldsymbol{D}_1$ and $\boldsymbol{D}_2$ are M×M and (2N-1-M)×M, respectively. The propagator matrix $\boldsymbol{P}$, which is a unique linear operator, can be written as:

$$\boldsymbol{P}^{\mathrm{H}}\boldsymbol{D}_1 = \boldsymbol{D}_2. \tag{10}$$

Defining:

$$\boldsymbol{Q}^{\mathrm{H}} = [\boldsymbol{P}^{\mathrm{H}} \quad -\boldsymbol{I}_{2N-1-M}]. \tag{11}$$

According to (9) and (11):

$$\boldsymbol{Q}^{\mathrm{H}}\boldsymbol{D} = [\boldsymbol{P}^{\mathrm{H}} \quad -\boldsymbol{I}_{2N-1-M}]\begin{bmatrix}\boldsymbol{D}_1 \\ \boldsymbol{D}_2\end{bmatrix} = \boldsymbol{0}_{(2N-1-M)\times M}, \tag{12}$$

where $\boldsymbol{I}_{(2N-1-M)}$ is a (2N-1-M)×(2N-1-M) identity matrix. The equation (12) shows that the columns of $\boldsymbol{Q}$ are orthogonal to the extended steering vectors $\boldsymbol{d}(\theta)$ and the subspace of the $\boldsymbol{d}(\theta)$ is equal to the signal subspace. According to the orthogonal principle between the signal subspace and the noise subspace, the subspace of $\boldsymbol{Q}$ is equivalent to the noise subspace.

Now, the spatial spectrum of the PM algorithm is defined as:

$$p(\theta) = \frac{1}{\boldsymbol{d}^{\mathrm{H}}(\theta)\boldsymbol{Q}\boldsymbol{Q}^{\mathrm{H}}\boldsymbol{d}(\theta)}. \tag{13}$$

The key problem of the PM is how to estimate the propagator matrix $\boldsymbol{P}$ from the array manifold matrix. However, in real environments, the array manifold matrix is usually unknown. Obviously, it is known from equation (8) that the matrix $\boldsymbol{D}$ is included in the $\boldsymbol{R}_4$. Therefore, the propagator matrix $\boldsymbol{P}$ can be estimated by substituting $\boldsymbol{R}_4$ for $\boldsymbol{D}$. In order to improve the estimation accuracy, the reduced-dimension $\hat{\boldsymbol{R}}_4$ is partitioned into two submatrices:

$$\hat{\boldsymbol{R}}_4 = \begin{bmatrix}\hat{\boldsymbol{R}}_{41} \\ \hat{\boldsymbol{R}}_{42}\end{bmatrix}, \tag{14}$$

where the dimension of $\hat{\boldsymbol{R}}_{41}$ and $\hat{\boldsymbol{R}}_{42}$ are M×(2N-1) and (2N-1-M)×(2N-1), respectively, and then the estimated propagator matrix $\hat{\boldsymbol{P}}$ can be obtained by minimizing the cost function $\xi(\hat{\boldsymbol{P}})$:

$$\xi(\hat{\boldsymbol{P}}) = \left\| \hat{\boldsymbol{R}}_{42} - \hat{\boldsymbol{P}}^{\mathrm{H}}\hat{\boldsymbol{R}}_{41} \right\|_F^2, \tag{15}$$

where $\|\cdot\|_F$ indicates the Frobenius norm, and then the optimal solution $\hat{\boldsymbol{P}}$ is given by:

$$\hat{\boldsymbol{P}} = (\hat{\boldsymbol{R}}_{41}\hat{\boldsymbol{R}}_{41}^{\mathrm{H}})^{-1}\hat{\boldsymbol{R}}_{41}\hat{\boldsymbol{R}}_{42}^{\mathrm{H}}. \tag{16}$$

Then,

$$\hat{\boldsymbol{Q}}^{\mathrm{H}} = [\hat{\boldsymbol{P}}^{\mathrm{H}} \quad -\boldsymbol{I}_{2N-1-M}]. \tag{17}$$

The difference between PM and MUSIC algorithm is that the columns of $\hat{\boldsymbol{Q}}$ are not orthogonal. In order to introduce the orthogonalization, the orthonormalized matrix $\hat{\boldsymbol{Q}}_0$ is obtained as follows:

$$\hat{\boldsymbol{Q}}_0 = \hat{\boldsymbol{Q}}(\hat{\boldsymbol{Q}}^{\mathrm{H}}\hat{\boldsymbol{Q}})^{-1/2}. \quad (18)$$

Till now, the implementation of the proposed algorithm with finite array data can be summarized as follows:

Step 1 Estimate $\hat{\boldsymbol{C}}_4$ from the received data by (6).

Step 2 Obtain the reduced-dimension matrix $\hat{\boldsymbol{R}}_4$ by removing the redundant items of the expanded matrix $\hat{\boldsymbol{C}}_4$ according to (8).

Step 3 Achieve the linear operator $\hat{\boldsymbol{P}}$ according to (15) and (16), and then calculate the orthonormalized matrix $\hat{\boldsymbol{Q}}_0$ based on (18).

Step 4 Estimate the DOAs of source signals with the help of the following spatial spectrum $\hat{p}_0(\theta)$.

$$\hat{p}_0(\theta) = \frac{1}{\boldsymbol{d}^{\mathrm{H}}(\theta)\hat{\boldsymbol{Q}}_0\hat{\boldsymbol{Q}}_0{}^{\mathrm{H}}\boldsymbol{d}(\theta)}. \quad (19)$$

C. Complexity analysis

Regarding the computational complexity, we only consider the major part, which involves in cumulant matrix construction, the linear operation, EVD implementation and one-dimensional (1-D) spectrum-peak searching. The computational complexity of proposed algorithm is analyzed in comparison with the MFOC-MUSIC algorithm [14]. For MFOC-MUSIC algorithm, the major computations involved are to calculate the $N^2\times N^2$ cumulant matrix $\boldsymbol{C}_4$, to perform EVD of the reduced-dimension $(2N\text{-}1)\times(2N\text{-}1)$ cumulant matrix $\boldsymbol{R}_4$ and to perform 1-D spectrum-peak searching. Therefore, the computational complexity of the MFOC-MUSIC algorithm is $O((9N^4L)+(4/3)(2N\text{-}1)^3+(180/\Delta\theta)(2N\text{-}1)^2)$, where L and $\Delta\theta$ denote the number of snapshots and the scanning interval, respectively. For proposed MFOC-OPM algorithm, the major computational complexity is to form one $N^2\times N^2$ cumulant matrix $\boldsymbol{C}_4$ and perform the linear operator on the reduced-dimension $(2N\text{-}1)\times(2N\text{-}1)$ cumulant matrix $\boldsymbol{R}_4$, since it doesn't require EVD and spectrum-peak searching. Therefore, the computational complexity of the proposed algorithm is $O((9N^4L)+(M(2N\text{-}1)^2))$. From the analysis above, it is obvious that the proposed algorithm has lower computational cost than the MFOC-MUSIC algorithm, especially when the number of sensors and snapshots increases.

IV. SIMULATION RESULTS

In this section, simulation results are provided to validate the effectiveness of the proposed algorithm both in spatially-white noise and spatially-color noise environments, respectively. A three-element ULA (N=3) with $\lambda/2$ spacing is employed. Consider three mutually independent far-field source signals (M=3) coming from {-20°, 20°, 45°}. The noise is assumed to be spatial white or color complex Gaussian, and the SNR is defined relative to each source signal. The mentioned algorithms are carried out by 500 independent Monte-Carlo trials. Two performance indices, called normalized probability of success (NPS) and average estimate variance (AEV), are defined to evaluate the performance of the two algorithms:

$$\mathrm{AEV} = \frac{\sum_{i=1}^{M}\mathrm{var}\,\hat{\theta}_i}{M},\ i=1,\cdots M \quad (20)$$

$$\mathrm{NPS} = \frac{\Upsilon_{suc}}{\mathrm{T}_{total}} \quad (21)$$

where $\hat{\theta}_i$ is the estimate of real θ_i. The Υ_{suc} and T_{total} denote the times of success and Monte-Carlo trial, respectively. Furthermore, a successful experiment is that satisfies $\max(|\hat{\theta}_i-\theta_i|)<\varepsilon$, and ε equals 0.8 and 1.6 for comparison versus SNR and snapshot, respectively.

Experiment 1: AEV and NPS versus SNR

In the first experiment, we examine the performance of the proposed algorithm against SNR. The number of snapshots L is 2000, and the SNR is varied from 5 to 25 dB. Figures 1 and 2 show the AEV of the DOAs estimation against input SNR in both spatially-white noise and spatially-color noise environments, respectively. It can be observed from Figs. 1 and 2 that the MFOC-OPM provides almost the same performance as the MFOC-MUSIC algorithm at low SNR. Figure 3 displays the NPS of the DOAs estimation against the SNR. Similar to Figs. 1 and 2, Fig. 3 achieves a similar performance to the MFOC-MUSIC algorithm even if at low SNR. Moreover, as the SNR increases, the performance curves of each figure tend to become consistent. Although the MFOC-OPM performs quite like MFOC-MUSIC algorithm at low, medium and high SNR, the computational complexity of the proposed method is significantly lower than that of the MFOC-MUSIC algorithm. The reason is that the proposed algorithm doesn't require EVD and spectrum-peak searching.

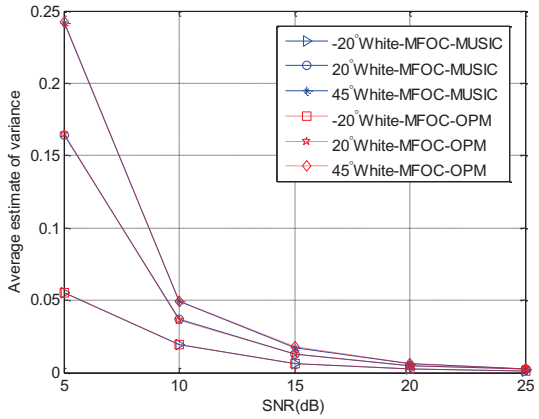

Fig. 1. AEV comparisons versus SNR in white situation.

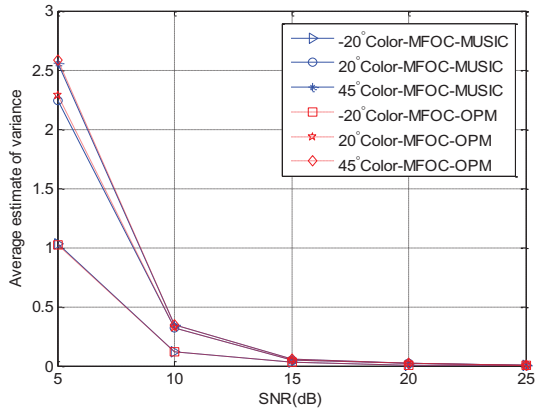

Fig. 2. AEV comparisons versus SNR in color situation.

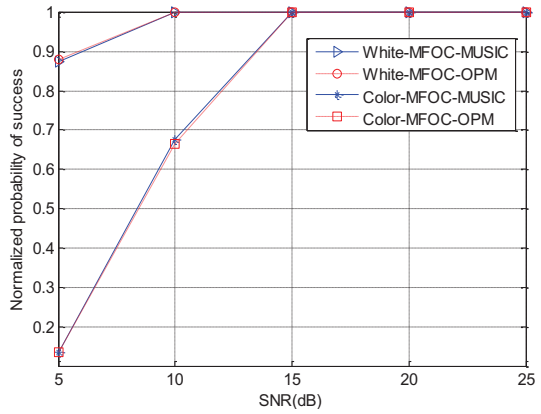

Fig. 3. NPS comparisons versus SNR.

Experiment 2: AEV and NPS versus snapshots

In the second experiment, we consider the same scenario as the first one at different number of snapshots. When the SNR is set to be 10 dB, the performance curves of AEV and NPS versus the number of snapshots in both spatially-white noise, and spatially-color noise environments are plotted in Figs. 4, 5 and 6, respectively. It can be seen from Figs. 4, 5 and 6 that the performance of the MFOC-OPM is approximately identical to that of the MFOC-MUSIC algorithm at low SNR. Furthermore, due to the small snapshots case, the curves of the two algorithms display sharp fluctuation as the number of snapshots is varied from 400 to 800. Moreover, Figs. 4, 5 and 6 illustrate the performance of the two algorithms under the white noise situation is better than that of the color noise situation. As the snapshots increases, the performance curves of each figure tend to become stabilized. Therefore, we can come to a conclusion that the estimated performance of the MFOC-OPM and MFOC-MUSIC algorithms becomes optimal when the snapshots number goes to infinity. However, as the analysis given in section III.C, the complexity of the MFOC-OPM is obviously smaller than that of the MFOC-MUSIC algorithm, and the convergence speed of the MFOC-OPM is much faster than that of the MFOC-MUSIC algorithm due to without using EVD and spectrum-peak searching. The merit of the proposed algorithm lies in the simple and efficient implementation in comparison to the MFOC-MUSIC algorithm.

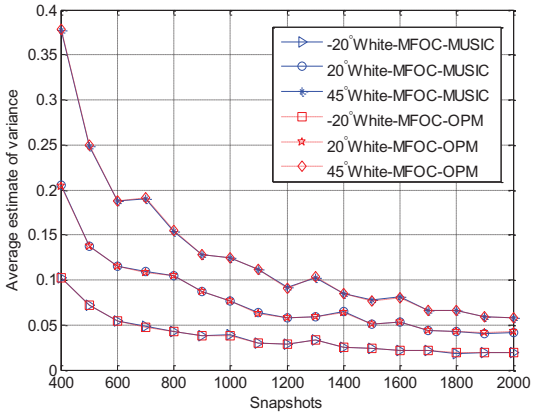

Fig. 4. AEV comparisons versus snapshots in white situation.

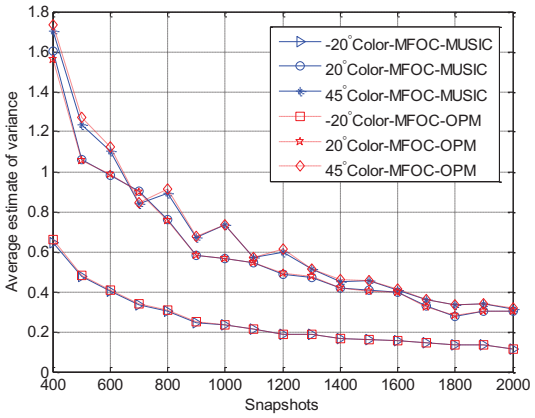

Fig. 5. AEV comparisons versus snapshots in color situation.

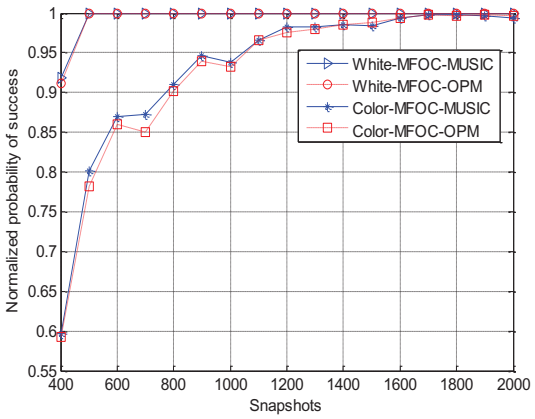

Fig. 6. NPS comparisons versus snapshots.

Experiment 3: Computational complexity versus number of sensors and snapshots

In the last experiment, the computational burden required by the proposed algorithm is compared with the MFOC-MUSIC algorithm. The number of the source signals is set to be M=3. For MFOC-MUSIC algorithm, the scanning interval is defined as $\Delta\theta$=0.01. Figure 7 shows the computational complexity of the two algorithms as a function of the number of sensors (from N=3 to N=10) when the number of snapshots is L=50. Figure 8 shows the computational complexity of the two algorithms as a function of the number of snapshots (from L=100 to L=1000) when the number of sensors is N=3. Figures 7 and 8 clearly show that the proposed algorithm achieves less computational load than MFOC-MUSIC algorithm as the number of sensors and snapshots increases, respectively. This is consistent with the theoretical analysis given in Section III.C.

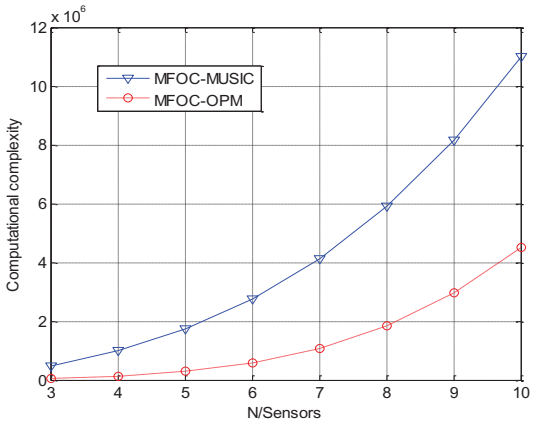

Fig. 7. Computational complexity comparison versus the number of sensors.

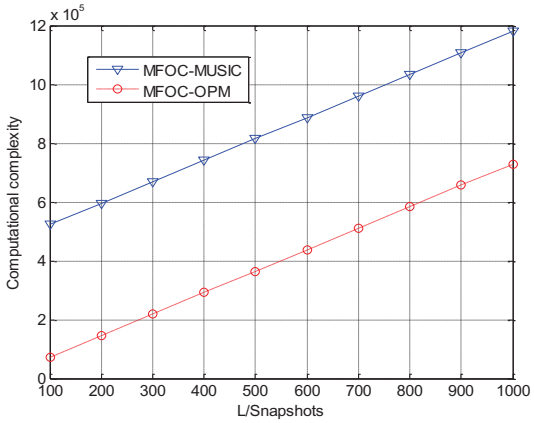

Fig. 8. Computational complexity comparison versus the number of snapshots.

V. CONCLUSION

In this paper, a low complexity DOA estimation algorithm called the MFOC-OPM has been proposed. In the proposed algorithm, the extended effective array aperture can resolve the number of sources more than or equal to that of the array elements, and the proposed algorithm can almost perform like MFOC-MUSIC algorithm especially in low SNR and small number of snapshots. Moreover, the proposed algorithm has the advantage of reduced computational load due to the fact that it doesn't require EVD and spectrum-peak to obtain its signal subspace and noise subspace. Therefore, such an advantage is highly desirable for practical applications when the low-computational cost and highly real-time data process are required. Simulation results demonstrate the effectiveness of the proposed algorithm both in spatially-white noise and in spatially-color noise environments.

ACKNOWLEDGMENT

This work was supported partially by the National Natural Science Foundation of China (no. 61002010) and the project of the State Key Laboratory of Millimeter Waves (no. K201314).

REFERENCES

[1] H. Krim and M. Viberg, "Two decades of array signal processing research: the parametric approach," *IEEE Signal Processing Magazine*, vol. 13, no. 4, pp. 67-94, Jul. 1996.

[2] I. Bekkerman and J. Tabrikian, "Target detection and localization using MIMO radars and sonars," *IEEE Trans. Signal Process.*, vol. 54, no. 10, pp. 3873-3883, 2006.

[3] R. O. Schmidt, "Multiple emitter location and signal parameter estimation," *IEEE Trans. Antennas and Propagation*, vol. 34, no. 3, pp. 276-280, Mar. 1986.

[4] E. M. Al-Ardi, R. M. Shubair, and M. E. Al-Mualla, "Direction of arrival estimation in a multipath environment: an overview and a new contribution," *Applied Computational Electromagnetics Society Journal*, vol. 21, no. 3, pp. 226-239, Nov. 2006.

[5] R. Roy and T. Kailath, "ESPRIT-estimation of signal parameters via rotational invariance techniques," *IEEE Trans. Acoust. Speech Signal Process*, vol. 37, no. 7, pp. 984-995, Jul. 1989.

[6] C. Qian, L. Huang, and H. C. So, "Computationally efficient ESPRIT algorithm for direction-of-arrival estimation based on Nyström method," *Signal Process.*, vol. 94, no. 1, pp. 74-80, 2014.

[7] M. L. McCloud and L. L. Scharf, "A new subspace

identification algorithm for high resolution DOA estimation," *IEEE Trans. Antennas Propag.*, vol. 10, no. 50, pp. 1382-1390, 2002.

[8] H. Changuel, A. Changuel, and A. Gharsallah, "A new method for estimating the direction-of-arrival waves by an iterative subspace-based method," *Applied Computational Electromagnetics Society Journal*, vol. 25, no. 5, pp. 476-485, May 2010.

[9] W. J. Zeng, X. L. Li, and X. D. Zhang, "Direction -of-arrival estimation based on the joint diagonalization structure of multiple fourth-order cumulant matrices," *IEEE Signal Processing Letters*, vol. 16, no. 3, pp. 164-167, 2009.

[10] B. Porat and B. Friedlander, "Direction finding algorithms based on high-order statistics," *IEEE Trans. Signal Process.*, vol. 39, no. 1, pp. 2016-2025, 1991.

[11] J. Munier and G. Y. Delisle, "Spatial analysis using new properties of the cross-spectral matrix," *IEEE Trans. on Signal Processing*, vol. 39, no. 3, pp. 746-749, 1991.

[12] A. Li and S. Wang, "Propagator method for DOA estimation using fourth-order cumulant," *Wireless Communications, Networking and Mobile Computing (WiCOM), 2011 7th International Conference on*, Wuhan, China, pp. 1-4, 2011.

[13] S. Marcos, A. Marsal, and M. Benidir, "The propagator method for source bearing estimation," *Signal Processing*, vol. 42, no. 2, pp. 121-138, 1995.

[14] P. Palanisamy and N. Rao, "Direction of arrival estimation based on fourth-order cumulant using propagator method," *Progress In Electromagnetics Research B*, vol. 18, pp. 83-99, 2009.

[15] P. Chevalier, L. Albera, A. Ferreol, and P. Comon, "On the virtual array concept for the fourth-order array processing," *IEEE Trans. Signal Process.*, vol. 53, no. 4, pp. 1254-1271, 2005.

[16] J. H. Tang, X. C. Si, and P. Chu, "Improved MUSIC algorithm based on fourth-order cumulants," *Systems Engineering and Electronics*, vol. 32, no. 2, pp. 256-259, 2010.

[17] P. Chevalier and A. Ferreol, "On the virtual array concept for the fourth-order direction finding problem," *IEEE Transactions on Signal Processing*, vol. 47, no. 9, pp. 2592-2595, 1999.

Heping Shi received the B.S. and M.S. degrees from Tianjin University of Technology and Education, China, in 2009 and 2012, respecttively. He is now a Ph.D. candidate at Tianjin University. His research interest is in the area of direction-of-arrival (DOA) and array signal processing.

Wen Leng received the B.S. degree and M.S. degrees from Northwestern Polytechnical University and Tianjin University in 1989 and 1992, respectively. He is currently a Lecturer in Tianjin University. His current research interests include Wireless data transmission, smart antenna, array signal processing, etc.

Anguo Wang received the Ph.D. degree from Tianjin University, China, in 2001. He is currently a Professor of Electronic Information Engineering with Tianjin University. He has co-authored over 80 scientific papers. His current research interests include communication system, smart antenna, microwave circuit, etc.

Hua Chen received the B.S. and the M.S. degree from Tianjin University, China, in 2010 and 2013, respecttively. He is now a Ph.D. candidate at Tianjin University. His research interests include image processing and direction-of-arrival (DOA).

Yuchu Ji received the B.S. and M.S. degrees from China University of Mining & Technology, Xuzhou, China, in 2008 and 2011, respectively. He is currently a Lecturer in Civil Aviation University of China. His research interests include cooperation communication and space time coding techniques.